

Article

A Mathematical Model for the Action Spectrum of Steady-State Pupil Size in Photopic Vision with Insight into Healthful Lighting

Shuxiao Wang ^{1,2,*} , Jianping Zhao ², Lixiong Wang ^{1,*}, Wenye Hu ³  and Fanfang Yan ⁴¹ School of Architecture, Tianjin University, 92nd Weijinlu, Nankai District, Tianjin 300072, China² China Academy of Building Research, 30th Beisanhuandonglu, Chaoyang District, Beijing 100033, China³ School of Architecture, Design and Planning, The University of Sydney, Sydney, NSW 2006, Australia⁴ Department of Psychology, University of Chinese Academy of Sciences, Beijing 100049, China

* Correspondence: wangshuxiao417@163.com (S.W.); wangshuxiao@chinaibee.com (L.W.)

Abstract: The pupillary light reflex, which has been seen as an important noninvasive and objective indicator of autonomic nervous system function, can be used for evaluating the impact of different lighting conditions in buildings on circadian behaviors, assessing ipRGC function in healthy and diseased retinas, and explaining luminance adaptation. However, the mechanism by which the intrinsic and extrinsic signals of ipRGCs regulate the steady-state pupil size under continuous lighting stimuli is still not clearly understood after decades of exploration. This paper presents a new experimental protocol with a large hemisphere LED screen as the stimulation device, allowing for a more realistic and comprehensive study in architectural spaces, which can potentially inform the design of lighting systems in buildings that promote healthy vision and comfort. Results reveal that both intrinsic and extrinsic signals participated in the process of regulating pupil size under continuous lighting conditions. Based on the findings, a new mathematical model was further proposed to calculate the contribution of these two signal sources to the changing intensity of melanopic radiance. The research outcomes also provide new insight into the mechanism of visual perception and adaptation and the nonvisual effect of eyes under different light conditions. Results suggest that the contribution of extrinsic signals may have been underestimated in previous studies since the extrinsic signal increases with reducing intensity in photopic conditions with lower melanopic radiance.

Keywords: ipRGCs; light adaptation; nonvisual effect; action spectrum; human-centric lighting



Citation: Wang, S.; Zhao, J.; Wang, L.; Hu, W.; Yan, F. A Mathematical Model for the Action Spectrum of Steady-State Pupil Size in Photopic Vision with Insight into Healthful Lighting. *Buildings* **2023**, *13*, 781. <https://doi.org/10.3390/buildings13030781>

Academic Editor: Cinzia Buratti

Received: 7 February 2023

Revised: 8 March 2023

Accepted: 14 March 2023

Published: 16 March 2023



Copyright: © 2023 by the authors. Licensee MDPI, Basel, Switzerland. This article is an open access article distributed under the terms and conditions of the Creative Commons Attribution (CC BY) license (<https://creativecommons.org/licenses/by/4.0/>).

1. Introduction

The pupillary light reflex (PLR) is a reflex that controls the size of the pupil in response to the intensity of light falling on the retina. The pupil diameter mainly depends on the adaptation luminance [1]. The PLR has been seen as an important noninvasive indicator of autonomic nervous system function [2]. Historically, it was assumed that the PLR is driven by pathways originating in conventional photoreceptors [3]. Extensive efforts have been made, during the last century, to develop equations and mathematical models to predict pupil sizes under different lighting conditions. Based on a number of equations proposed, Watson and Yellott developed a unified formula for steady-state pupil size, considering photopic luminance as a controlling variable [4]. However, several observations have shown that $V(\lambda)$ -weighted indicators do not predict the PLR very well [5–7]. It is still unclear how the visual system is able to detect absolute changes in environmental irradiance to mediate the PLR [8].

In the early 2000s, the discovery of intrinsically photosensitive retinal ganglion cells (ipRGCs), which have extensive projections in the shell of the olivary pretectal nucleus (OPN) for mediating the PLR, may provide us with new insight into explaining this question [9–12]. Similar to other types of RGCs, ipRGCs also receive extrinsic signals

from rods and cones, in addition to their own intrinsic signal [13–15]. For longer stimuli durations, during the first 200 ms after the onset of incremental light stimuli, the initial constriction of the pupil is mediated solely by classical photoreceptors [16], after which the pupil gradually increases to a relatively stable state because of the light adaptation for classical photoreceptors and the involvement of melanopsin if the light intensity is higher than the threshold of melanopsin [17]. The contribution of melanopsin is the determining factor for the post-illumination pupil response (PIPR), i.e., sustained pupil constriction no less than 1.7 s after offset stimuli, when the stimuli are higher than the threshold of melanopsin [18]. Rao, Chan, and Zhu pointed out a limitation in earlier studies that did not account for the contribution of ipRGCs on pupil responses in those equations. To address this issue, Rao's team conducted an experiment to predict pupil size according to photopic and circadian luminance. Circadian luminance is the summation of the spectral irradiance of the light weighted by the circadian spectral sensitivity, which represents the spectral sensitivity of the third retinal input in addition to photopic and scotopic vision [19]. As Rao, Chan, and Zhu's experiment was designed for typical computer and smartphone screens, the luminance tested was limited to a range from 50 cd/m² to 300 cd/m². In architectural spaces, it is not uncommon that luminance could be lower than this range. Spitschan also suggested that a larger range of luminance under natural behavior with conjoint spectral measurement needs to be considered in future studies [20]. Additionally, the light stimuli used in their research were relatively small (covering a circular field of 20 deg of the participants' visual field), while larger stimuli are usually expected in a typical lighting environment in architectural spaces, which plays a crucial role in influencing human visual comfort, performance, productivity, and overall wellbeing. Therefore, this present research explored the relationship between pupil sizes and different photoreceptors with a wider luminance range, color-mixing LED spectra, and much larger stimulus size.

The individual contribution of different photoreceptors to the sustained state of pupillary constriction during continuous light stimuli is still unclear. Some research supports that the melanopsin signal is the sole source of the sustained response 30 s after the onset of the stimuli [21–23], and some results suggest that in primates, the role of the melanopsin signal is to combine with the cone signal over the photopic range, serving to maintain pupil constriction during continuous daylight illumination [24–26]. Spitschan developed a function of pupil size with melanopic retinal intensity, which has a much better prediction than Watson and Yellott's formula. He reported that there is a notable and systematic deviation for the 670 nm data points [20]. However, his research was based on an extant data set described in Bouma's research [6]. In this paper, we present experiments for exploratory research to develop a mathematical model of the individual contributions of different photoreceptors to the sustained state of pupillary constriction. The data collected in this research could provide new empirical evidence.

2. Methods

2.1. Participants

It has been demonstrated that pupillary diameter can be significantly influenced by non-photopic factors such as diseases such as glaucoma [27], sleep quality [28], state of arousal [5], type of cognitive activities [29], and environmental factors [30,31].

Five male participants (mean age = 30, SD = 4.2) took part in this research. They all reported having normal corrected visual acuity and normal color vision. None of the participants had health issues, such as sleep disorders influencing pupil constriction. Written informed consent was obtained from each observer prior to this study. This study was approved by the Institutional Review Board of the Institute of Psychology, Chinese Academy of Sciences, and followed the tenets of the Declaration of Helsinki. During the experiment, all participants were asked to avoid caffeine and alcohol one day before the experiment, a prescription medication known to influence the PLR. All the participants were asked to have a sleep duration of no less than 7 h the day before the experiment and to keep their mood in peace during the experiment.

2.2. Apparatus

In this research, we developed a simulation facility with a hemisphere LED screen to present uniform stimuli with different spectra and intensities for the participants, as shown in Figure 1. The technical characteristics of the LED screen are listed in Table 1, and Figure 2 presents the relative spectral intensity of R/G/B chips used in the LED screen, with a comparison to the melanopic action spectrum given in CIE/S 026 [10]. Compared to the stimulation devices used in related research, the LED hemisphere can tune the luminance and spectrum in any direction in the full visual field of the participants. During the experiments, participants positioned their chins on the adjustable chin rest so that one of their eyes was located on the center point of the hemisphere, with the eye tracker monitoring the pupil size during the experiment, as shown in Figure 1.

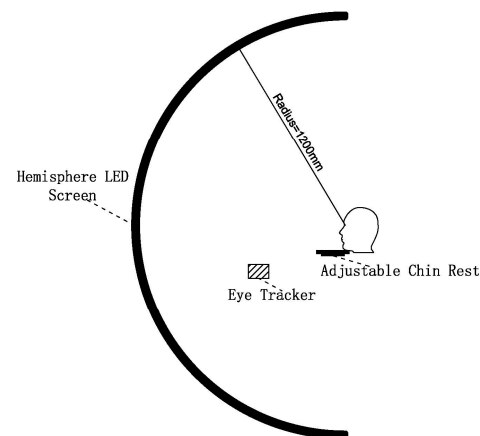


Figure 1. Schematic diagram of the apparatus during the experiment (unit: mm).

Table 1. Technical characteristics of the hemisphere LED Screen.

Characteristics	Performance
Diameter	2.4 m
Number of pixels	723,360 pixels
Color	R/G/B
Maximum luminance	>1000 cd/m ²
Luminance uniformity	>95%
Refresh rate	≥2000 Hz
Bit depth	12 bit

An infrared eye tracker aSee Pro F90 (produced by 7 invensun Technology Co., Ltd., Beijing, China) was used in this research, the sampling rate of which was 100 Hz. The claimed test error of the pupil diameter of this instrument is no more than 1.5%. A SPIC-300 Spectral Irradiance Colorimeter produced by EVERFINE Cooperation (Hangzhou, China), an illuminance meter, and an L1009 luminance meter produced by LMT LICHTMESSTECHNIK GMBH (Berlin, Germany) were used to calibrate the stimulus of the experiment. All these instruments were calibrated by the National Institute of Metrology, China.

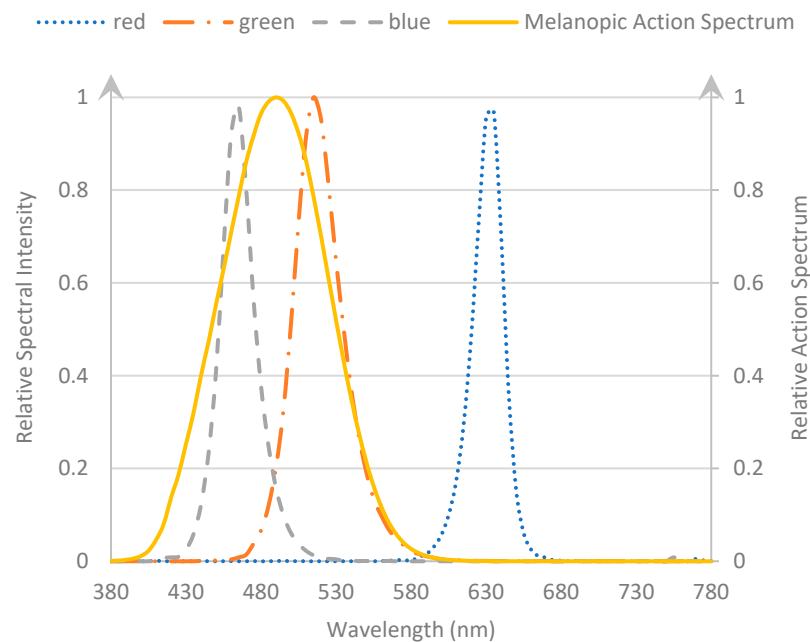


Figure 2. Relative spectral intensity of R/G/B chips used in the LED screen.

2.3. Experiment Protocol

The baseline pupil diameter (BPD) was defined as the average pupil diameter over 30 s pre-stimulus phase. The relative pupil diameter was the measured pupil diameter normalized to the BPD, avoiding any individual difference in pupil size [32]. The PIPR was determined as the relative pupil diameter 6 s after the offset of stimuli, which has a strong dependence on the melanopsin signal.

All experiments were conducted at 10 am and 5 pm to minimize the potential error due to the circadian phase [33]. The PLR was measured under undilated conditions. The light stimuli described in 2.4 were presented sequentially. The measurements of every stimulus were preceded by 20 min of dark adaptation in the laboratory (the vertical illuminance on the eye of the participant was less than 0.001 lux) to guarantee the full dark adaptation of rods and cones [17]. The baseline pupil diameter was measured in the dark during 30 s of fixation before the onset of light stimuli. The participants were instructed to gaze at the center point of the screen, and no specified cognitive task was required. The pupillary light response to the stimuli presented for one minute in duration was monitored simultaneously. We set the time the stimulus offset as 0 s and the stimulus onset as -60 s. The PIPR was recorded for 30 s after the stimulus offset.

2.4. Stimuli

To develop the mathematical model of the individual contributions of intrinsic signals and external signals to the steady-state PLR under a continuous stimulus, eight types of spectra were used, including red, green, blue, and polychromatic white light, with five different CCTs, as shown in Figure 3. Nine levels and twelve levels of intensity were set for monochromatic light and white light, respectively, as shown in Table 2.

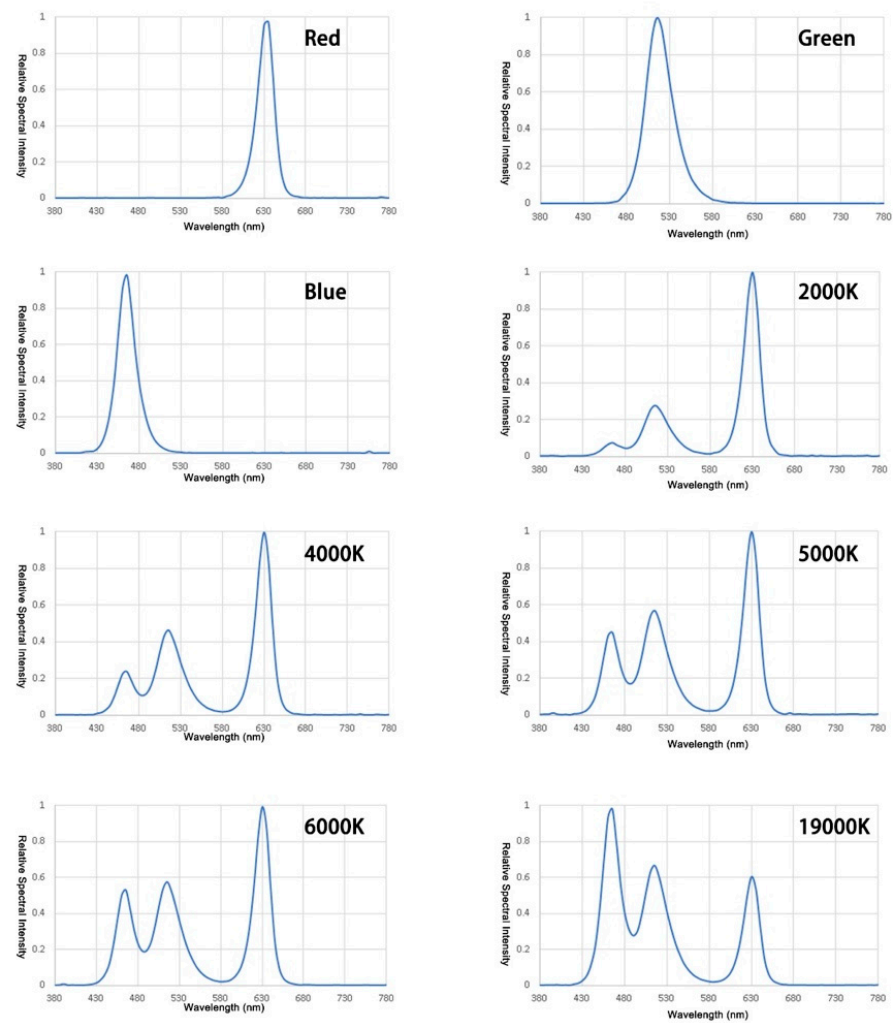


Figure 3. The eight spectra of the experimental scenarios.

Table 2. Detailed information on the scenarios for the experiment.

Scenario NO.	Color/CCT	Measured Luminance (cd/m ²)	Melanopic Radiance (W/m ² /Sr)	Scenario No.	Color/CCT	Measured Luminance (cd/m ²)	Melanopic Radiance (W/m ² /Sr)
1	Red	5	0.000	45	3642	104	0.085
2	Red	13	0.000	46	3594	151	0.117
3	Red	28	0.000	47	3574	208	0.158
4	Red	52	0.000	48	3599	266	0.217
5	Red	82	0.000	49	3619	323	0.250
6	Red	131	0.000	50	3755	448	0.326
7	Red	189	0.001	51	3744	505	0.389
8	Red	261	0.001	52	6685	11	0.010
9	Red	366	0.001	53	6462	18	0.017
10	Green	18	0.017	54	6148	26	0.025

Table 2. Cont.

Scenario NO.	Color/CCT	Measured Luminance (cd/m ²)	Melanopic Radiance (W/m ² /Sr)	Scenario No.	Color/CCT	Measured Luminance (cd/m ²)	Melanopic Radiance (W/m ² /Sr)
11	Green	46	0.045	55	5833	44	0.040
12	Green	101	0.098	56	5429	69	0.063
13	Green	187	0.180	57	5385	95	0.095
14	Green	310	0.299	58	5270	153	0.135
15	Green	477	0.460	59	5168	220	0.187
16	Green	691	0.665	60	5188	285	0.246
17	Green	961	0.926	61	5192	354	0.300
18	Green	1353	1.303	62	5280	503	0.466
19	Blue	5	0.035	63	5350	649	0.619
20	Blue	7	0.057	64	7095	10	0.010
21	Blue	16	0.124	65	6959	19	0.019
22	Blue	30	0.230	66	6406	29	0.031
23	Blue	50	0.382	67	6026	50	0.051
24	Blue	77	0.587	68	5749	68	0.067
25	Blue	112	0.851	69	5757	102	0.103
26	Blue	156	1.184	70	5648	147	0.147
27	Blue	220	1.672	71	5571	202	0.196
28	4336	10	0.007	72	5671	263	0.264
29	3193	19	0.012	73	5832	302	0.302
30	2951	29	0.019	74	5740	446	0.467
31	2734	53	0.034	75	5874	536	0.533
32	2440	72	0.044	76	11,091	9	0.011
33	2123	122	0.062	77	12,717	14	0.019
34	2190	153	0.086	78	14,339	21	0.028
35	2152	211	0.110	79	16,877	35	0.049
36	2126	270	0.148	80	19,003	55	0.079
37	2099	307	0.167	81	19,739	74	0.106
38	2080	462	0.246	82	19,560	123	0.177
39	2101	508	0.268	83	19,430	175	0.254
40	5545	10	0.009	84	19,457	229	0.337
41	4979	18	0.019	85	19,756	287	0.403
42	4302	32	0.027	86	19,652	403	0.591
43	3836	53	0.039	87	19,613	540	0.804
44	3854	70	0.059	—	—	—	—

3. Results

3.1. Verifying the Contribution of the Intrinsic Signal and External Signal to the Steady State of PLR

As Gooley claimed, during exposure to a 30–60 min continuous light stimulus, because of the slower decreasing relative contribution of cones to the PLR, pupillary size continued to dilate to a steady state after the initial constriction, which was an order of magnitude longer than previously reported. The time course of the PLR under continuous stimulus was first examined to develop a method of calculating the steady-state pupil size. Results showed that pupil sizes could reach the balance state in seconds after light onset, and the slope of the response curve vs. time before the stimuli offset became flat, as shown in Figure 4.

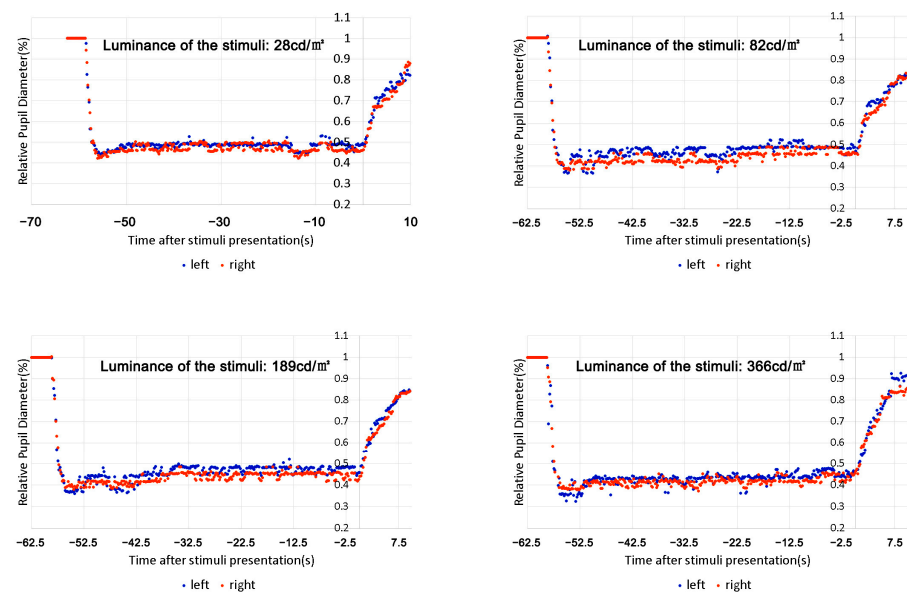


Figure 4. Average pupillograms of the five participants under the red stimulus, as an example, with different luminance.

Comparisons of relative pupil diameters (RPDs) at different times after the stimuli presentation showed that the mean difference of RPDs was not significant after the first 10 s of exposure to light. Table 3 demonstrates an example of RPD comparisons under red stimuli with a luminance of 366 cd/m². The RPD at each time point was compared with the RPD at any other time point to identify any statistically significant differences. Interestingly, the phenomenon of ‘pupillary escape’ reported by Gooley was not observed in this experiment, even for the red stimulus without activating melanopsin [21]. In our experiment, there is a significant difference between the RPD at 1 s after stimulus onset and other subsequent RPDs, but no significant difference was found for RPDs with light exposure longer than 11 s. This suggests that at the very beginning of stimulus onset, there is a transient response that is followed by a gradual relaxation in the pupil to a more sustained and balanced state after 11 s of light exposure. Therefore, the average RPD from 11 s after the stimulus onset until light-off can be taken as the steady-state pupil size.

Table 3. Paired comparisons of RPDs at different times after stimuli presentation (the luminance of red stimuli is 366 cd/m²). Dependent factor: Relative pupil diameter.

LSD			
(I) Time after the Stimulus Onset	(J) Time after the Stimulus Onset	Mean Difference (I–J)	Sig.
1.00	11.00	0.42839 *	0.000
	21.00	0.42766 *	0.000
	31.00	0.42221 *	0.000
	41.00	0.42215 *	0.000
	55.00	0.41890 *	0.000
11.00	1.00	−0.42839 *	0.000
	21.00	−0.00073	0.980
	31.00	−0.00618	0.831
	41.00	−0.00624	0.829
	55.00	−0.00949	0.743
21.00	1.00	−0.42766 *	0.000
	11.00	0.00073	0.980
	31.00	−0.00545	0.851
	41.00	−0.00551	0.849
	55.00	−0.00875	0.762
31	1.00	−0.42221 *	0.000
	11.00	0.00618	0.831
	21.00	0.00545	0.851
	41.00	−0.00006	0.998
	55.00	−0.00331	0.909
41.00	1.00	−0.42215 *	0.000
	11.00	0.00624	0.829
	21.00	0.00551	0.849
	31.00	0.00006	0.998
	55.00	−0.00324	0.911
55.00	1.00	−0.41890 *	0.000
	11.00	0.00949	0.743
	21.00	0.00875	0.762
	31.00	0.00331	0.909
	41.00	0.00324	0.911

* The mean difference is significant at the 0.05 level.

As shown in Figure 5, the steady-state pupil size under red and blue stimuli both decreased significantly with increasing stimulus intensity (for red stimuli: $F = 506.955$, $P = 0$, blue stimuli: $F = 2169.339$, $P = 0$). There was an interesting phenomenon that the steady-state pupil size under the red stimuli had a saturation effect, which means that the pupil diameter did not decrease with the increasing intensity when the mean difference in pupil size had no significant difference between stimuli with a luminance of 189 cd/m² and 366 cd/m² (Table 4). However, the minimum pupil size of the blue stimulus (mean value = 0.3107) was significantly smaller than that of the red stimulus (mean value = 0.4331) ($F = 2707.161$, $P = 0$).

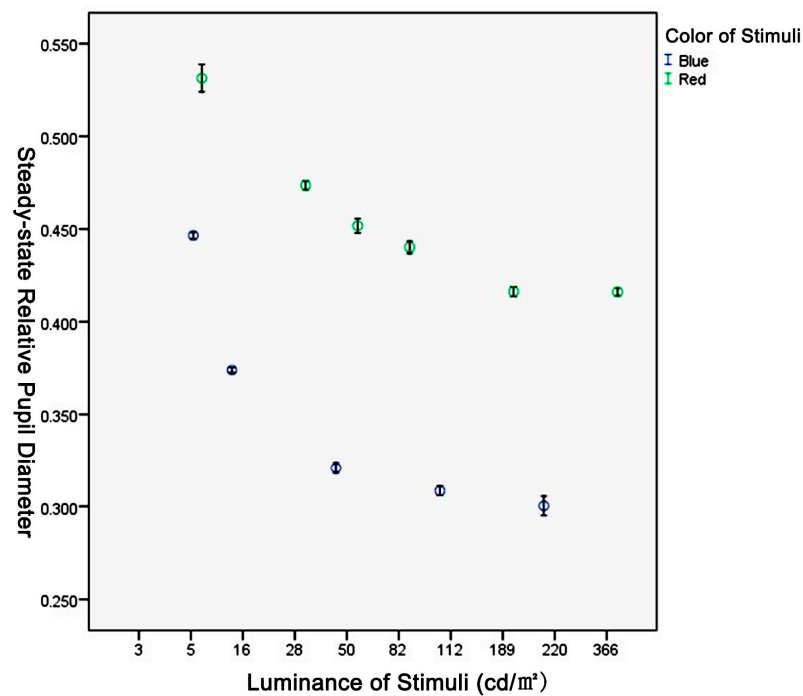


Figure 5. Comparison of steady-state pupil size under different luminance of the red (shown as green circles) and blue stimuli (shown as blue circles).

Table 4. Comparisons of steady-state RPDs for the red stimulus with different luminance.

Dependent Factor: Relative Pupil Diameter						
LSD						
(I) Luminance of Stimulus (cd/m ²)	(J) Luminance of Stimulus (cd/m ²)	Mean Difference (I–J)	Std. Error	Sig.	95% Confidence Interval Lower Bound	95% Confidence Interval Upper Bound
5	28	0.05306 *	0.003044	00.000	0.04708	0.05903
	82	0.08648 *	0.003033	0.000	0.08052	0.09243
	189	0.11041 *	0.003033	0.000	0.10446	0.11636
	366	0.11060 *	0.003037	0.000	0.10464	0.11655
28	5	−0.05306 *	0.003044	0.000	−0.05903	−0.04708
	82	0.03342 *	0.003129	0.000	0.02728	0.03956
	189	0.05736 *	0.003129	0.000	0.05122	0.06349
	366	0.05754 *	0.003132	0.000	0.05140	0.06369
82	5	−0.08648 *	0.003033	0.000	−0.09243	−0.08052
	28	−0.03342 *	0.003129	0.000	−0.03956	−0.02728
	189	0.02394 *	0.003118	0.000	0.01782	0.03005
	366	0.02412 *	0.003122	0.000	0.01800	0.03025
189	5	−0.11041 *	0.003033	0.000	−0.11636	−0.10446
	28	−0.05736 *	0.003129	0.000	−0.06349	−0.05122
	82	−0.02394 *	0.003118	0.000	−0.03005	−0.01782
	366	0.00019	0.003122	0.953	−0.00594	0.00631
366	5	−0.11060 *	0.003037	0.000	−0.11655	−0.10464
	28	−0.05754 *	0.003132	0.000	−0.06369	−0.05140
	82	−0.02412 *	0.003122	0.000	−0.03025	−0.01800
	189	−0.00019	0.003122	0.953	−0.00631	0.00594

* The mean difference is significant at the 0.05 level.

3.2. Development of a Mathematical Model for the Action Spectrum of Steady-State Pupil Size in Photopic Vision

Both McDougal and Gooley supported that the pupil size dilated after the initial constriction over time because of the light adaptation of cones in a relatively long-time course, and the contribution of cones to the PLR could be ignored after a specified time of exposure [3,34]. In this experiment, the response of pupils to red stimuli of different intensities was investigated with the blue stimulus as a reference. According to Table 2, red spectra only stimulated the cones in photopic conditions without activating melanopsin. From the data, unexpectedly, we did not find a slow recovery process, instead, a fast establishment of the steady-state PLR in seconds was found. Therefore, melanopsin might not be the sole source for mediating the PLR function but in cooperating with cones.

Another phenomenon found in this research was the saturation effect of the PLR under red stimulus when a pupil was not reached its minimum state. A possible reason for this was that cones reach their saturation state without adjusting their sensitivity by light adaptation [35]. This phenomenon might further confirm that melanopsin functions analogously to a photographer's light meter, providing a measure to regulate functional adaptation in the mammalian retina [36,37]. According to Prigge and Mark, M1 ipRGCs send signals retrogradely to dopaminergic amacrine cells (DACs) within the retina, providing a possible mechanism by which ipRGCs may influence light adaptation via the retinal dopaminergic system [36,38]. Therefore, we hypothesized that the melanopsin signal might have two functions: one is that the signal could be sent to the brain to mediate pupil size directly; the other is that it could mediate the extrinsic signal of cones by adjusting their sensitivity and deliver it to the brain to regulate the pupil indirectly, as shown in Figure 6.

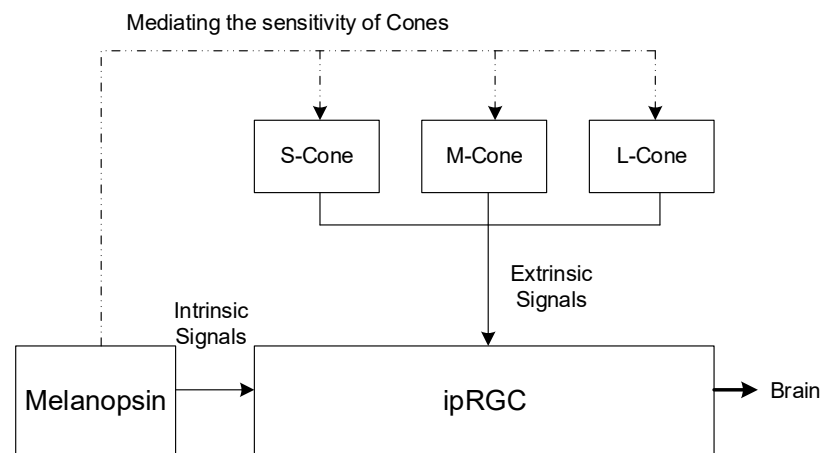


Figure 6. Hypotheses for the mechanism of pupil mediation with different signals.

Most existing models developed from sensory to light are based on S-shaped curves, which are mathematically more accurately referred to as a hyperbolic tangent (tanh) curve [35,39,40]. Therefore, the PLR under continuous light stimulus may be expressed as the following formula:

$$PLR = k_1 f_1(mel) + k_2 f_2(mel, L) + k_3 \quad (1)$$

where k_1 , k_2 , and k_3 are constants.

$f_1(mel)$ is the response of melanopsin on melanopic radiance mel as a function of the direct component of the intrinsic signal on the PLR, which can be expressed as follows:

$$f_1(mel) = \frac{a}{1 + c \cdot e^{b \cdot mel}} + d \quad (2)$$

where a , b , c , and d are constants.

$f_2(mel, L)$ is the response of cones on stimulus luminance L with the gain control changing as determined by the intrinsic signal on the PLR, and $f_1(mel)$ can be seen as a proportionality constant under the specific adaptation state [41]. So, it can be expressed as Equation (3):

$$f_2(mel, L) = \frac{g}{1 + h \cdot e^{m \cdot L \cdot f_1(mel)}} \quad (3)$$

where g , h , and m are constants.

As the PIPR is highly dependent on the intrinsic signal from melanopsin, we can take the PIPR as the dependent variable, perform regression of Equation (2) first, and then substitute Equation (1) as:

$$PLR = k_1 \cdot PIPR + k_2 \frac{g}{1 + h \cdot e^{m \cdot L \cdot PIPR}} + k_3 \quad (4)$$

From the steady-state pupil diameter data collected under 87 scenarios listed in Table 2, we found that the $V(\lambda)$ -weighted luminance did not predict the steady-state pupil size well, and there was a significant difference in pupil sizes under stimuli with the same luminance of different spectra (Figure 7). Melanopic radiance could provide a much better explanation, especially for the higher melanopic radiance situations, but deviation increased in the lower melanopic radiance region (melanopic radiance lower than $0.01 \text{ W/m}^2/\text{Sr}$), particularly with red spectra (Figure 8). This reconfirmed that both cones and melanopsin contributed to the PLR activities under continuous stimulus in photopic conditions, as Manuel stated [20]. Manuel's findings were based on the reanalysis of Bouma's data set, which was published in 1962 when ipRGCs were not yet discovered.

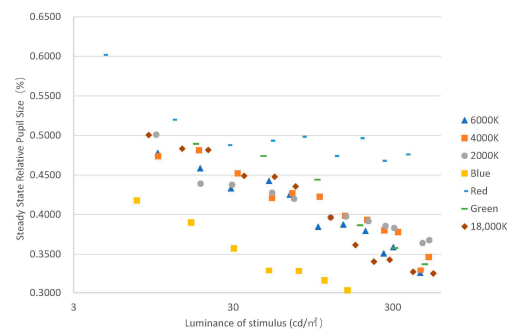


Figure 7. Steady-State of Pupil Diameter vs. Luminance of Stimulus (log scale).

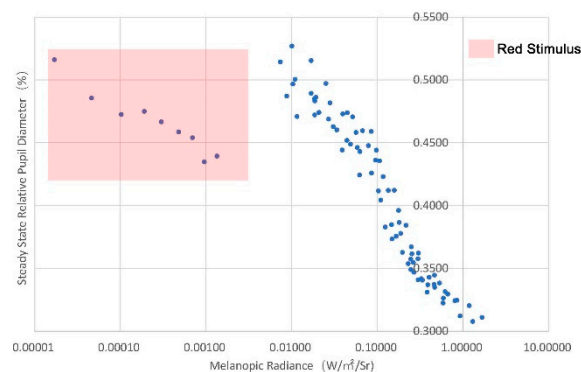


Figure 8. Measured Steady-State of Pupil Diameter vs. Melanopic Radiance of Stimulus (log scale).

A new model to establish the relationship between the PIPR and melanopic radiance was proposed by performing a nonlinear regression model using SPSS, Version 23. The constants in Equation (2) were determined, and the model can be expressed as:

$$PIPR = \frac{0.481}{1 + 0.649 \cdot e^{10.095 \cdot mel}} + 0.501 \quad (5)$$

The best model was identified for its ability to fit the result of the PIPR very well with a high value of $R^2 = 0.818$ (as shown in Table 5). It can be seen from the mathematical model of the PIPR that melanopsin has a higher sensation threshold value, approximately 0.001 W/m^2 , in a situation with uniform luminance distribution in the visual field of participants on the level of 1 cd/m^2 with a 6000 K spectrum, as specified in Figure 9.

Table 5. ANOVA of the PIPR Regression.

Source	Sum of Squares	df	Mean Squares
Regression	38.364	4	9.591
Residual	0.231	83	0.003
Uncorrected Total	38.594	87	
Corrected Total	1.271	86	

Dependent variable: PIPR. $R^2 = 1 - (\text{Residual Sum of Squares})/(\text{Corrected Sum of Squares}) = 0.818$.

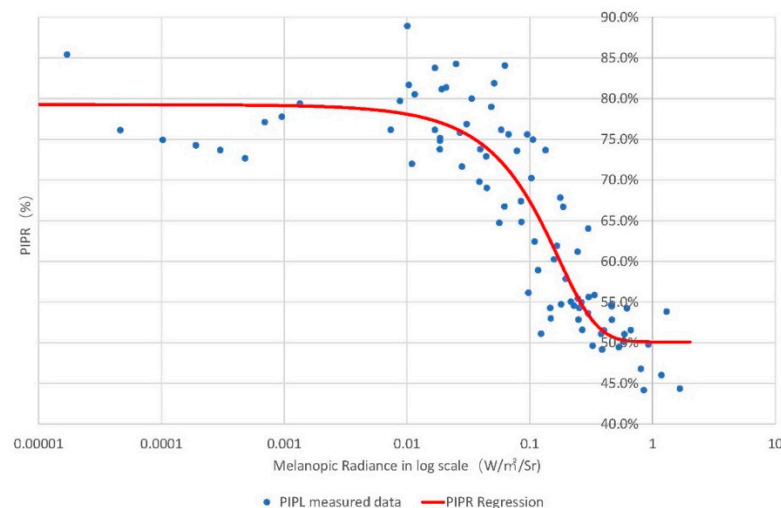


Figure 9. A regression model was developed using PIPR measurements as a function of melanopic radiance (in a logarithmic scale). The normalized PIPR values are represented with blue dots and the regression curve is shown in red. The model yields a high goodness of fit (0.818).

With the function of SPSS nonlinear regression, the constant in Equation (4) was determined for predicting the steady-state PLR with PIPR calculated using Equation (5) and measured luminance as follows:

$$PLR = 0.552 \cdot PIPR - \frac{1120.801}{1 - 24690.191e^{(L \times PIPR)}} + 0.051 \quad (6)$$

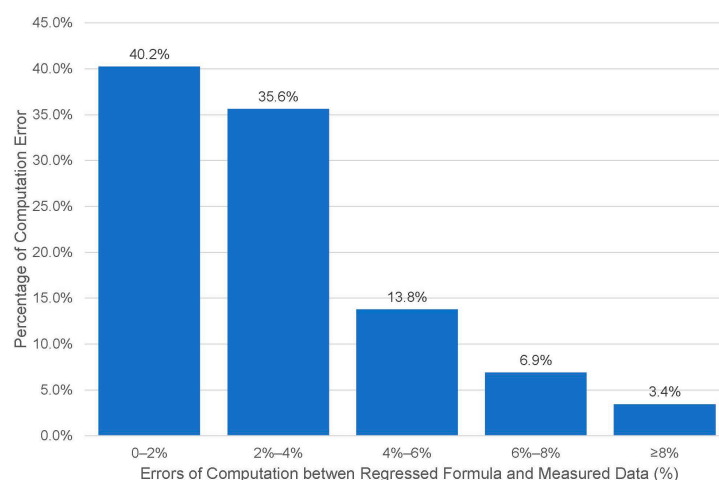
The best model was identified for its ability to fit the result of the relative steady-state PLR with a high value of $R^2 = 0.930$ (Table 6). This also reconfirmed the hypothesis that both intrinsic signals from melanopsin and mediated extrinsic signals from cones mediated by intrinsic signals co-mediate PLR function under continuous light stimulus higher than the threshold value of melanopsin.

Table 6. ANOVA of the PLP Regression.

Source	Sum of Squares	df	Mean Squares
Regression	15.145	4	3.786
Residual	0.024	83	0.000
Uncorrected Total	15.169	87	
Corrected Total	0.342	86	

Dependent variable: PIPR. $R^2 = 1 - (\text{Residual Sum of Squares}) / (\text{Corrected Sum of Squares}) = 0.930$.

More than 75% of the absolute values of errors between the computed results and measured values are less than 4%, and the average value is 3% (see Figure 10).

**Figure 10.** Distribution of computation error between the regressed model and measured data.

3.3. Explanation for the Mathematic Model

With Equation (6), the relative steady-state PLR can be calculated under a continuous light stimulus with different intensities and spectra (Figure 11). For stimuli with lower intensities (less than 10 cd/m^2), the calculated PLR values for different spectra are very close, but the deviation grows with the increasing luminance of the stimulus. In this paper, we proposed a new term daylight (D65) coefficient of the PLR, which is defined as the ratio of the luminance of test stimuli and the luminance produced by radiation conforming to standard daylight (D65) that provides an equal PLR with the stimuli. The daylight (D65) coefficients of the PLR for different spectra with different luminance levels were further calculated. For a higher intensity of the stimulus, the daylight (D65) coefficient of the PLR is a constant with a value the same as the melanopic daylight (D65) efficacy ratio determined according to CIE S/026:2018, which means that the intrinsic signal from melanopsin can be seen as the sole source for steady-state PLR mediation. However, when the intensity of the stimulus is lower than a critical value, the daylight (D65) coefficient of the PLR changes with decreasing stimulus intensity, approaching 1. This means that both intrinsic and extrinsic signals contribute to the function of mediating the PLR under continuous light presentation, but their respective contributions dynamically change with the intensity of the stimulus, which is very similar to the situation of mesopic vision.

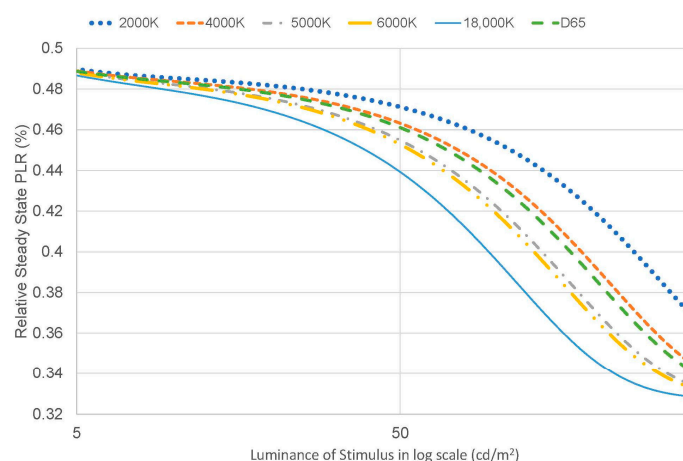


Figure 11. Calculated relative steady-state PLR with Formula (6) vs. luminance of stimulus with different spectra.

4. Discussion and Conclusions

The PLR can be seen as a valuable indicator of autonomic nervous system function and is widely used as a noninvasive tool for basic neuroscience research, physiological and psychological clinical diagnosis, etc. The PLR has been widely investigated in humans [42], and some consensus has been made on signal sources for mediating the initial constriction of pupils and the PIPR, but we are still uncertain about the mechanism by which the intrinsic and extrinsic signals of ipRGCs regulate the steady-state pupil size under continuous lighting stimuli. In this paper, two experiments were conducted, and we confirmed the following:

- (1) We did not find continued dilation of the pupil size after the initial constriction under continuous light presentation for a relatively long time (up to 30 min) but found that the pupil size could reach balance in no more than 10 s, even under a red stimulus that only activated the cones. This suggests that both intrinsic and extrinsic signals participated in the process of regulating pupil size under continuous lighting conditions, unlike the previous report indicating an underestimated contribution of extrinsic signals [21–23].
- (2) The contribution of the signals might change with the intensity of melanopic radiance. For melanopic radiance with higher intensity, the intrinsic signal solely determines the pupil size under sustained light presentation, which is consistent with the data from Manuel [20]; however, for photopic conditions with lower melanopic radiance, the contribution of the intrinsic signal decreases, and the extrinsic signal increases with reducing intensity (see Figure 12).
- (3) The hypothesis for the potential function of melanopsin in regulating the sensitivity of cones was proposed and verified according to the two experiments. This hypothesis is also supported by the research of Prigge and Mark, who found that M1 ipRGCs, which also regulate the function OPN for the PLR and SCN for behavior, send signals retrogradely to dopaminergic amacrine cells (DACs) within the retina, providing a possible mechanism by which ipRGCs may influence light adaptation via the retinal dopaminergic system [36,38,43]. This may provide new insight into how to explain the mechanism of visual perception.

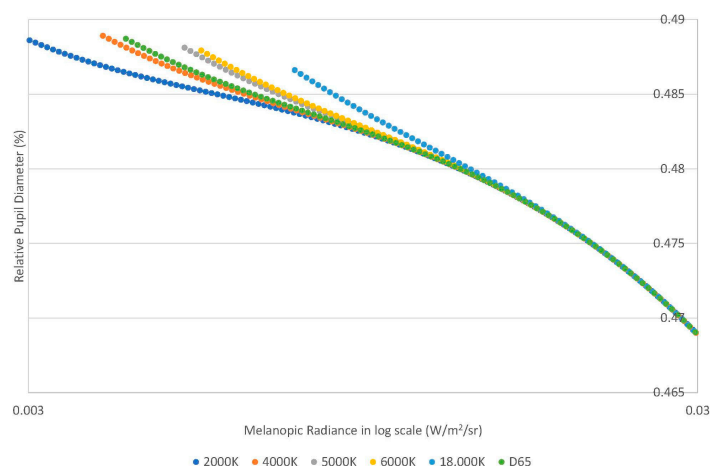


Figure 12. Calculated Steady-State of Pupil Diameter with Formula (6) vs. Melanopic Radiance of Stimulus (log scale).

In this research, we have drawn some preliminary conclusions from the two experiments with a relatively small number of male participants, but there is still a long way to go to develop a complicated model of the PLR under different spectra and luminance distributions for people of different ages and genders. The current findings provide new insights into the mechanisms underlying visual perception, such as light adaptation, and the contribution of signals to light perception.

Additionally, this research presents a novel non-invasive method for investigating the non-visual effect of light. As an easily measurable physiological marker, pupil responses can be a promising tool for further research and accelerate the implementation of research findings into practical solutions for improving human health and wellbeing.

Research on the PLR may provide some new implications for the following topics:

- (1) As M1 ipRGCs are responsible for both the circadian clock and the PLR, research on the PLR might offer us a quick and easy tool to evaluate the impact of different lighting conditions on the nonvisual effect of eyes, such as circadian behaviors.
- (2) Many studies have shown that ipRGC dysfunction may have strong relevance to human diseases such as Alzheimer's disease, Parkinson's disease, diabetic retinopathy, glaucoma, etc. [44]. Research on the PLR may develop a standard protocol for pupillometry as an emerging method for the direct assessment of ipRGC function in healthy and diseased retinas, which may be used for early detection and clinical examination of these ipRGC-related diseases.
- (3) The measurement or estimation of adaptation levels in natural environments with a complex luminance distribution is a very important topic, but there have been no studies directly dealing with this issue [45]. Historically, the steady-state PLR has been seen as an indicator for luminance adaptation, but recent studies on ipRGCs offered us a better mechanistic explanation of the relationship between light adaptation of the visual system and the PLR. This suggests that the same class of ipRGCs for the PLR also functions analogously to a photographer's light meter, providing a measure to regulate luminance adaptation by synapsing with bipolar and amacrine cells [36,37,46]. Research on the PLR might give us a new perspective on developing a model for light adaptation in a natural environment.

Author Contributions: Conceptualization and Project Administration, S.W. and F.Y.; Methodology, J.Z. and L.W.; Validation, W.H.; Writing—original draft, S.W.; writing—review and editing, W.H., J.Z. and L.W.; funding acquisition, J.Z.; supervision, L.W. and J.Z. All authors have read and agreed to the published version of the manuscript.

Funding: This research was funded by the National Key R&D Program of China (2018YFC0705100), Space Medical Experiment Project of China Manned Space Program (HYZHXM03004).

Data Availability Statement: The data presented in this study are available on request from the corresponding author.

Acknowledgments: We would like to thank Kees Teunissen for helpful comments on the manuscript.

Conflicts of Interest: The authors declare no conflict of interest.

References

1. David, L.D.; Kevin, W.H.; Richard, G.M.; Steffy, G.R. *The Lighting Handbook*, 10th ed.; Illuminating Engineering Society: New York, NY, USA, 2011.
2. Hall, C.A.; Chilcott, R.P. Eyeing up the Future of the Pupillary Light Reflex in Neurodiagnostics. *Diagnostics* **2018**, *8*, 19. [[CrossRef](#)] [[PubMed](#)]
3. McDougal, D.H.; Gamlin, P.D. The influence of intrinsically-photosensitive retinal ganglion cells on the spectral sensitivity and response dynamics of the human pupillary light reflex. *Vis. Res.* **2010**, *50*, 72–87. [[CrossRef](#)]
4. Watson, A.B.; Yellott, J.I. A unified formula for light-adapted pupil size. *J. Vis.* **2012**, *12*, 12. [[CrossRef](#)]
5. Berman, S.; Fein, G.; Jewett, D.; Saika, G.; Ashford, F. Spectral Determinants of Steady-State Pupil Size with Full Field of View. *J. Illum. Eng. Soc.* **1992**, *21*, 3–13. [[CrossRef](#)]
6. Bouma, H. Size of the Static Pupil as a Function of Wave-length and Luminosity of the Light Incident on the Human Eye. *Nature* **1962**, *193*, 690–691. [[CrossRef](#)]
7. Lucas, R.J.; Douglas, R.H.; Foster, R.G. Characterization of an ocular photopigment capable of driving pupillary constriction in mice. *Nat. Neurosci.* **2001**, *4*, 621–626. [[CrossRef](#)]
8. Joyce, D.S. Temporal, Spatial and Adaptation Characteristics of Melanopsin Inputs to the Human Pupil Light Reflex. Ph.D. Thesis, Queensland University of Technology, Brisbane City, QLD, Australia, 2016.
9. Berson, D.M. Strange vision: Ganglion cells as circadian photoreceptors. *Trends Neurosci.* **2003**, *26*, 314–320. [[CrossRef](#)]
10. CIE S 026/E:2018; CIE System for Metrology of Optical Radiation for IpRGC-Influenced Responses to Light. Commission Internationale De L'eclairage(Cie) CIE: Vienna, Austria, 2018.
11. Dacey, D.; Liao, H.; Peterson, B.; Robinson, F.; Smith, V.; Pokorny, J.; Yau, K.-W.; Gamlin, P.D. Melanopsin-expressing ganglion cells in primate retina signal color and irradiance and project to the lgn. *Nature* **2005**, *433*, 749–754. [[CrossRef](#)]
12. Wang, S.; Zhao, J. New perspectives on light adaptation of visual system research with the emerging knowledge on non-imageforming effect. *Front. Built Environ.* **2022**, *8*, 1019460. [[CrossRef](#)]
13. Berson, D.M.; Dunn, F.A.; Takao, M. Phototransduction by Retinal Ganglion Cells That Set the Circadian Clock. *Science* **2002**, *295*, 1070–1073. [[CrossRef](#)] [[PubMed](#)]
14. Hattar, S.; Liao, H.-W.; Takao, M.; Berson, D.M.; Yau, K.-W. Melanopsin-containing retinal ganglion cells: Architecture, projections, and intrinsic photosensitivity. *Science* **2002**, *295*, 1065–1070. [[CrossRef](#)]
15. Hattar, S.; Lucas, R.J.; Mrosovsky, N.; Thompson, S.; Douglas, R.H.; Hankins, M.W.; Lem, J.; Biel, M.; Hofmann, F.; Foster, R.G.; et al. Melanopsin and rod–cone photoreceptive systems account for all major accessory visual functions in mice. *Nature* **2003**, *424*, 75–81. [[CrossRef](#)]
16. Zele, A.J.; Feigl, B.; Adhikari, P.; Maynard, M.L.; Cao, D. Melanopsin photoreception contributes to human visual detection, temporal and colour processing. *Sci. Rep.* **2018**, *8*, 3842. [[CrossRef](#)] [[PubMed](#)]
17. Münch, M.; Léon, L.; Crippa, S.V.; Kawasaki, A. Circadian and Wake-Dependent Effects on the Pupil Light Reflex in Response to Narrow-Bandwidth Light Pulses. *Investig. Ophthalmol. Vis. Sci.* **2012**, *53*, 4546–4555. [[CrossRef](#)] [[PubMed](#)]
18. Adhikari, P.; Feigl, B.; Zele, A.J. Rhodopsin and Melanopsin Contributions to the Early Redilation Phase of the Post-Illumination Pupil Response (PIPR). *PLoS ONE* **2016**, *11*, e0161175. [[CrossRef](#)] [[PubMed](#)]
19. Rao, F.; Chan, A.; Zhu, X.-F. Effects of photopic and cirtopic illumination on steady state pupil sizes. *Vis. Res.* **2017**, *137*, 24–28. [[CrossRef](#)]
20. Spitschan, M. Photoreceptor inputs to pupil control. *J. Vis.* **2019**, *19*, 5. [[CrossRef](#)] [[PubMed](#)]
21. Gooley, J.J.; Mien, I.H.; Hilaire, M.A.S.; Yeo, S.C.; Chua, E.C.P.; Van Reen, E.; Hanley, C.J.; Hull, J.T.; Czeisler, C.A.; Lockley, S.W. Melanopsin and Rod-Cone Photoreceptors Play Different Roles in Mediating Pupillary Light Responses during Exposure to Continuous Light in Humans. *J. Neurosci. Off. J. Soc. Neurosci.* **2012**, *32*, 14242–14253. [[CrossRef](#)]
22. Park, J.C.; Moura, A.L.; Raza, A.S.; Rhee, D.W.; Kardon, R.H.; Hood, D.C. Toward a Clinical Protocol for Assessing Rod, Cone, and Melanopsin Contributions to the Human Pupil Response. *Investig. Ophthalmology Vis. Sci.* **2011**, *52*, 6624–6635. [[CrossRef](#)]
23. Gamlin, P.D.; McDougal, D.H.; Pokorny, J.; Smith, V.C.; Yau, K.-W.; Dacey, D.M. Human and macaque pupil responses driven by melanopsin-containing retinal ganglion cells. *Vis. Res.* **2007**, *47*, 946–954. [[CrossRef](#)]
24. Drouyer, E.; Rieux, C.; Hut, R.A.; Cooper, H.M. Responses of Suprachiasmatic Nucleus Neurons to Light and Dark Adaptation: Relative Contributions of Melanopsin and Rod–Cone Inputs. *J. Neurosci.* **2007**, *27*, 9623–9631. [[CrossRef](#)]
25. Wong, K.Y.; Dunn, F.A.; Graham, D.M.; Berson, D.M. Synaptic influences on rat ganglion-cell photoreceptors. *J. Physiol.* **2007**, *582*, 279–296. [[CrossRef](#)]
26. Lucas, R.J. Diminished Pupillary Light Reflex at High Irradiances in Melanopsin-Knockout Mice. *Science* **2003**, *299*, 245–247. [[CrossRef](#)]

27. Zhang, H.; Guo, J.; Wang, S. Clinical Nursing of Correlation between Pupil Changes and Diseases. *Chin. Gen. Pract. Nurs.* **2014**, *12*, 1123–1124. (In Chinese)
28. McDougal, D.H.; Gamlin, P.D.R. Pupillary Control Pathways. In *The Senses: A Comprehensive Reference*; Academic Press: New York, NY, USA, 2008; pp. 521–536.
29. Yu, Y.; Jiang, Y.; Wang, Y.; Yu, M. Pupil size as a biomarker of Memory Processing. *Adv. Psychol. Sci.* **2020**, *28*, 10. Available online: <http://kns.cnki.net/kcms/detail/11.4766.R.20200117.1029.012.html> (accessed on 5 January 2023). (In Chinese)
30. Dabbs, J.M. Testosterone and Pupillary Response to Auditory Sexual Stimuli. *Physiol. Behav.* **1997**, *62*, 909–912. [[CrossRef](#)]
31. Akashi, Y.; Muramatsu, R.; Kanaya, S. Unified Glare Rating (UGR) and subjective appraisal of discomfort glare. *Light. Res. Technol.* **1996**, *28*, 199–206. [[CrossRef](#)]
32. Sperandio, I.; Bond, N.; Binda, P. Pupil Size as a Gateway Into Conscious Interpretation of Brightness. *Front. Neurol.* **2018**, *9*, 1070. [[CrossRef](#)]
33. Zele, A.J.; Adhikari, P.; Cao, D.; Feigl, B. Melanopsin and Cone Photoreceptor Inputs to the Afferent Pupil Light Response. *Front. Neurol.* **2019**, *10*, 529. [[CrossRef](#)] [[PubMed](#)]
34. William, A.H.; Rushton, F.R.S. The Plotting of Dark-Adaptation Curves in Rod-Cone Investigations. *Am. J. Ophthalmol.* **1963**, *56*, 748–751.
35. Hung, G.K.; Ciuffreda, K.J. *Model of Visual System*; Kluwer Academic/Plenum Publishers: New York, NY, USA, 2002; pp. 125–127.
36. Hankins, M.W.; Hughes, S. Vision: Melanopsin as a novel irradiance detector at the heart of vision. *Curr. Biol.* **2014**, *24*, R1055–R1057.
37. Allen, A.E.; Storch, R.; Martial, F.P.; Petersen, R.S.; Montemurro, M.A.; Brown, T.M.; Lucas, R.J. Melanopsin-Driven Light Adaptation in Mouse Vision. *Curr. Biol.* **2014**, *24*, 2481–2490. [[CrossRef](#)]
38. Prigge, C.L.; Yeh, P.-T.; Liou, N.-F.; Lee, C.-C.; You, S.-F.; Liu, L.-L.; McNeill, D.S.; Chew, K.S.; Hattar, S.; Chen, S.-K.; et al. M1 ipRGCs Influence Visual Function through Retrograde Signaling in the Retina. *J. Neurosci.* **2016**, *36*, 7184–7197. [[CrossRef](#)]
39. Brainard, G.C.; Hanifin, J.P.; Greeson, J.; Byrne, B.; Glickman, G.; Gerner, E.; Rollag, M.D. Action Spectrum for Melatonin Regulation in Humans: Evidence for a Novel Circadian Photoreceptor. *J. Neurosci.* **2001**, *21*, 6405–6412. [[CrossRef](#)]
40. van Bommel, W. *Interior Lighting: Fundamentals, Technology and Application*; Springer International Publishing: Cham, Switzerland, 2019; p. 114.
41. Shapley, R.; Enroth-Cugell, C. Chapter 9 Visual adaptation and retinal gain controls. *Prog. Retin. Res.* **1984**, *3*, 263–346. [[CrossRef](#)]
42. Clarke, R.J.; Zhang, H.; Gamlin, P.D.R. Characteristics of the Pupillary Light Reflex in the Alert Rhesus Monkey. *J. Neurophysiol.* **2003**, *89*, 3179–3189. [[CrossRef](#)] [[PubMed](#)]
43. Schmidt, T.M.; Chen, S.-K.; Hattar, S. Intrinsically photosensitive retinal ganglion cells: Many subtypes, diverse functions. *Trends Neurosci.* **2011**, *34*, 572–580. [[CrossRef](#)] [[PubMed](#)]
44. Esquivia, G.; Hannibal, J. Melanopsin-expressing retinal ganglion cells in aging and disease. *Histol. Histopathol.* **2019**, *34*, 1299–1311. [[PubMed](#)]
45. International Commission On Illumination (CIE). *CIE 135/5:1999 Visual Adaptation to Complex Luminance*; CIE: Vienna, Austria, 1999.
46. Besenecker, U.C. Investigating Melanopsin Contribution to Scene Brightness Perception. Ph.D. Thesis, Rensselaer Polytechnic Institute, Troy, NY, USA, 2013.

Disclaimer/Publisher’s Note: The statements, opinions and data contained in all publications are solely those of the individual author(s) and contributor(s) and not of MDPI and/or the editor(s). MDPI and/or the editor(s) disclaim responsibility for any injury to people or property resulting from any ideas, methods, instructions or products referred to in the content.